

SETUP FOR THE NUCLOTRON BEAM TIME STRUCTURE MEASUREMENTS

A.Yu. Isupov^{†,‡,1}, V.P. Ladygin[†], and S.G. Reznikov[†]

[†] *Joint Institute for Nuclear Research, 141980 Dubna, Russia*

[‡] *E-mail: isupov@moonhe.jinr.ru*

Abstract

The setups for precise measurements of the time structure of Nuclotron internal and slowly extracted beams are described in both hardware and software aspects. The CAMAC hardware is based on the use of the standard CAMAC modules developed and manufactured at JINR. The data acquisition system software is implemented using the *ngdp* framework under the Unix-like operating system (OS) FreeBSD to allow the easy network distribution of the online data. It is demonstrated that the described setups are suitable for the continuous beam quality monitoring during the experiments performed at Nuclotron.

Keywords: CAMAC, data acquisition system, network distributed system, graphic user interface, beam time structure

PACS: 29.27.Fh, 07.05.Hd

¹Corresponding author.

Introduction

The experimental program at Nuclotron for heavy ion collisions [1, 2], few body [3] and polarization [4, 5] physics requires good quality of the internal and extracted beams. The time structure of the beam plays a crucial role in the experiments requiring high interaction rate. One of the parameters reflecting the beam time structure is the coefficient K_{dc} defined as

$$K_{dc} = \frac{1}{t_2 - t_1} \cdot \left[\int_{t_1}^{t_2} (dN/dt) dt \right]^2 / \left[\int_{t_1}^{t_2} (dN/dt)^2 dt \right], \quad (1)$$

where dN/dt is the beam current, $(t_2 - t_1) = T_{ext}$ is the time of the beam exposition. The real experiment requires that the K_{dc} coefficient should be about 0.85—0.95 for the efficient data taking.

Another problem of the experiment related with the beam time structure is the correct estimation of the data acquisition dead-time. This is important not only for the cross section evaluation, but also for the polarization measurements due to effect of the dead-time distortion [6]. For instance, large dead-time of the data acquisition (DAQ) due to oscillating interaction rate could significantly reduce the asymmetry values during the measurements of the analyzing powers [7, 8]. Such effect is especially important for the polarization measurements requiring the absolute normalization of the beam intensity or interaction rate in the wide range as in the TPD experiment on the measurements of the induced tensor polarization of deuteron beam travelling through matter [9, 10].

The Nuclotron internal target station (ITS) is an efficient tool to perform nuclear physics studies at energies from hundreds of MeV to several GeV per nucleon with both polarized and unpolarized beams [11]. However, in this case the useful events yield is the time dependent function of the beam and moving internal target interaction. Recently, new system of the ITS control and data acquisition has been developed [12]. In particular, the internal target mechanical vibrations were studied in details using this new system [12].

The Nuclotron extracted deuteron beam time structure has been studied previously during data taking of the TPD experiment [9, 10], on the measurements of the soft photons yield [13], and by the BM@N experiment [1]. The CAMAC and VME [14] based DAQ systems were used for the measurements performed at 4V [9, 10, 13] and 6V [1] beamlines, respectively. These measurements were performed in the trigger mode of the DAQ systems, when the information was read for each trigger. However, such mode cannot provide correct information on the beam time structure at high trigger rate due to dead-time distortion. These circumstances motivate us to organize the setup with negligible dead-time and to use it for the Nuclotron beam time structure measurements.

The goal of the paper is to report the details of the setups for the Nuclotron internal and extracted beam time structure measurements as well as first results obtained with deuteron, ${}^7\text{Li}$, and ${}^{12}\text{C}$ beams. The paper is organized in the following way. The chapter 1 contains the details of the hardware and software of the setups for the Nuclotron beam time structure investigations. The results on the extracted beam time structure are presented in chapter 2. The results on the investigation of the internal beam-target interaction are reported in chapter 3. The conclusions are drawn in the last chapter.

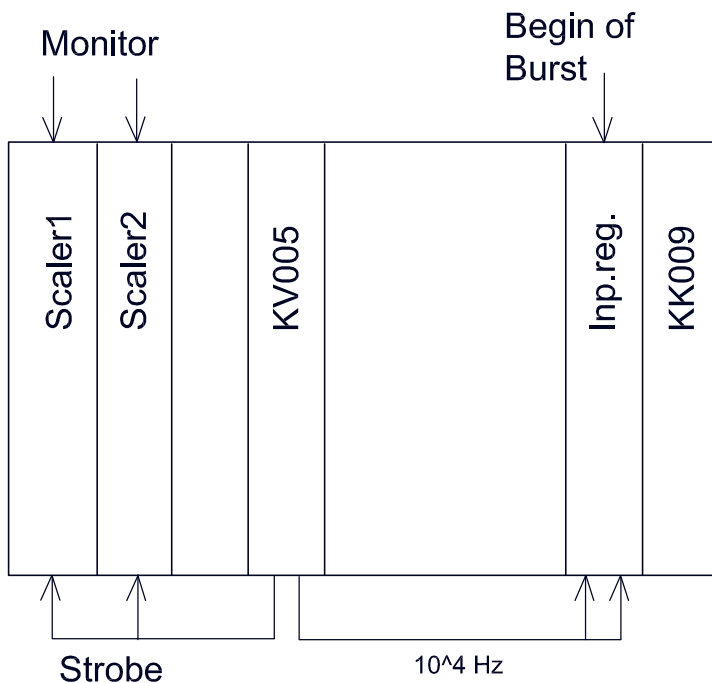


Figure 1: CAMAC hardware. See text for description.

1 Setup hardware and software

1.1 CAMAC electronics

Each setup contains input register, two identical scalars, and pulse generator CAMAC modules. Their functional scheme is outlined in Fig. 1. All CAMAC units were developed and produced at JINR. Both setups have the same modules disposition in the read-out crate.

The input register collects three inputs — accelerator cycle begin and two triggers — which lead to the LAM assertion. The input register is the only LAM source in the read-out crate, and the KK009 crate controller [15] is programmed to set the interrupt request (IRQ) at each LAM occurrence. Each of this IRQ leads to the invocation of the CAMAC interrupt handler function from the `spill` loadable kernel module (see chapter 1.2). Each of two triggers corresponds to scaler module should be read-out at current interrupt handler invocation. The two triggers should alternate strictly, so the Spill DAQ is able to handle improper trigger bit combinations and trigger sequences.

The KV005 [16] generator was used to produce the trigger signals sequence with the base frequency of 10^4 Hz, which corresponds to the time slice of $100 \mu\text{s}$.

The beam-target interaction intensity is measured by monitor scintillation counter, whose signal is split to fed the 0th input of both scalars. The odd scaler counts during odd time slice and is read-out during even one, and the even scaler — vice versa. This scheme allows us to avoid undercounts, only up to 1 pulse could be erroneously dropped or added in each time slice.

Because we read from scalars the least 16 bits only at each $100 \mu\text{s}$ time slice, the setups are able to consume counts with rate up to $\approx 6.5 \times 10^8$ Hz. This is more than

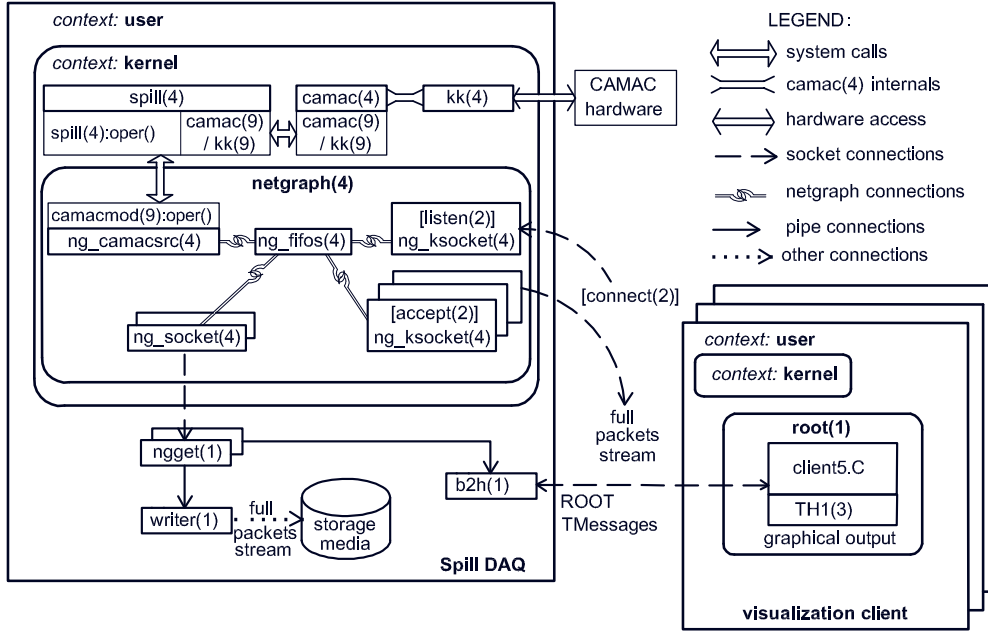


Figure 2: Overall Spill DAQ layout. See text for description.

enough because scalars are able to input up to $\approx (0.7 \div 1) \times 10^8$ Hz.

1.2 Spill DAQ system

Both setups have very similar software however each uses own hardware, in particular the main host. The overall Spill DAQ layout is pictured in Fig. 2, where we can see the main host under the FreeBSD OS as the rectangle entitled “Spill DAQ”, and optional hosts — as the rectangles “visualization client”. This main host deals with the CAMAC hardware using the PK009 ISA adapter for the KK009 CAMAC crate controller [15]. In the OS kernel context it has the *camac(4)* facility [17], *spill(4)* CAMAC kernel module, as well as the modules in the *netgraph(4)* package [18] style (Fig. 3). Fig. 3 shows the data streams transportation from the *spill(4)* CAMAC kernel module through the nodes, which are represented as rectangles with node name (up), type (left), and ID (right). The data streams are propagated along the graph edges, which are formed by pairs of connected hooks [18] (octagons in Fig. 3). The data are injected into graph by the *camacsrc* node and demultiplexed by the *ffos* node into more than one identical streams, which could be transferred both locally and remotely. In Fig. 2 we can see two of the data stream consumers: *writer(1)* and *b2h(1)*, whose standard inputs are fed by standard outputs of *ngget(1)* instances, which reads the *ffos* local outputs through the *netgraph* sockets provided by *ng_socket(4)* node instances. Each *ffos* output as well as their input could be connected and disconnected without disturbing other one(s). Due to *ffos* loading during the OS boot sequence all `load` user commands (see Table 1) are independent from each other. The “visualization client” in Fig. 2 executes one of the

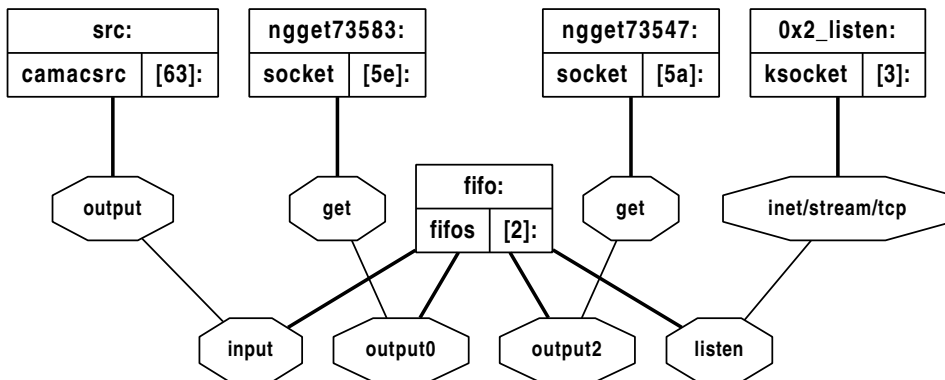


Figure 3: The Spill DAQ core is implemented by the *ngdp* graph. See text for description.

possible clients of the *b2h(1)* server — the ROOT script *client5.C*.

The *netgraph(4)* package [18] and *ngdp* framework [19, 20] involvement reduces the DAQ system implementation efforts essentially, because a number of software modules are ready to use: *ng_camacsrc(4)*, *ng_fifos(4)*, *ngget(1)* [20], *writer(1)* [21], *ng_ksocket(4)*, *ng_socket(4)*. The produced data could be distributed in form of both the *ngdp* packet stream(s) (for raw cycle-by-cycle ones) and ROOT framework [22] TMessages (for *b2h(1)* produced histograms). Specifically for the Spill DAQ we implement only the *spill(4)*, *spillconf(1)*, *spilloper(1)*, and *b2h(1)* software modules.

The *spill(4)* module is intended to work with the corresponding CAMAC hardware (see 1.1). It complies with requirements of the *camac(4)* and *ng_camacsrc(4)*, so implements the CAMAC interrupt handler function. This handler recognizes the following interrupt occurrences (events):

- begin of burst (BoB),
- odd and even trigger at end of 100 μ s time slice.

In total two data packet types are produced to contain as follows: *CYC_BEG* — the BoB timestamp, *CYC_END* — the read-out scaler data as the sequence of 50000 16-bit little-endian values to cover up to 5 s of burst. The *CYC_END* packet type is produced at obtaining the 50000th end-of-slice interrupt.

The CAMAC hardware description and handling are separated from the *spill(4)* module’s source and grouped together in the single *spill_hardware.h* header file. In the current implementation it uses macro interface *kk(9)* specific for the KK009 crate controller [15] instead of the crate controller independent one *camac(9)*, because the former interface allows us to perform each CAMAC cycle slightly faster [23].

The *spill(4)* module can be configured at startup by the *spillconf(8)* utility and controlled during operation by the *spilloper(8)* one. To operate with the Spill DAQ it has the configuration file (named by default *\$NGDPHOME/etc/spillsv.conf*) in the Makefile format (see also *make(1)*). This file establishes the correspondence between the user commands (“targets” in *make(1)* terminology) and actions which should be performed. This file is textual and could be revised easily. So typical user command look

Table 1: The user commands to control over Spill DAQ.

Command	Description
load	loads and configures the <i>spill(4)</i> and <code>ng_camacsrc</code> kernel modules, connects latter to <code>ng_fifos</code> input
unload	counterpart for previous
loadw	loads the <i>writer(1)</i> module and connects it to <code>ng_fifos</code> output. <code>RUNFILE</code> and <code>DATADIR</code> variables could be defined
unloadw	counterpart for previous
loadb2h	loads the <i>b2h(1)</i> module and connects it to <code>ng_fifos</code> output. <code>RUNFILE</code> variable could be defined
unloadb2h	counterpart for previous
continue	starts the handling of CAMAC interrupts
swstart	starts the handling of CAMAC interrupts with software BoB initiation by <i>callout(9)</i> mechanism
pause	counterpart for two previous
init	initializes the CAMAC hardware
finish	counterpart for previous
cleanall	resets all histograms in the <i>b2h(1)</i>
saveall	stores all <i>b2h(1)</i> histograms into ROOT TFile on hard disk (if <code>RUNFILE</code> variable was supplied for <code>loadb2h</code>)
disconn	disconnects all clients from <i>b2h(1)</i>
status	outputs status messages from present modules through <i>syslogd(8)</i>
seelog	starts the <i>syslogd(8)</i> output file <code>qdpblog</code> viewing by <i>tail(1)</i>

like the following:

```
make -f spillsv.conf RUNFILE=test loadw
```

All the defined user commands we summarize in the Table 1.

The *b2h(1)* (for “binary to histograms”) module is intended for ROOT histograms filling from the packet (binary) data representation obtained from `ng_fifos` node output. Due to simple nature of our setups we use the compiled-in histograms configuration from `hconf.h` header file. The 50000-bin histograms for at least last cycle and sum during current run, and optionally their Fourier transforms are booked at *b2h(1)* startup. At each `CYC_END` packet arrival these histograms and some statistics are updated. Namely, for 50 bins of 100 ms the mean of counts, its standard deviation, dispersion and dispersion

Table 2: The time structure characteristics for the Nuclotron slowly extracted beam.

Beam, T_{kin} (A·GeV)	K_{dc}	t_1 (ms)	t_2 (ms)	$\frac{\Delta N(\Delta f)}{0.5N_{\text{tot}}} (\%)$ for Δf as $f_1..f_2$ (Hz)					
				0..1	100..400	400..800	800..1200	1200..1600	1600..2000
d, 3.5	0.49	1000	2700	2.4	21.0	6.48	5.1	16.4	11.56
C, 3.5	0.218	900	2600	1.3	16.0	7.56	4.63	6.3	5.1
⁷ Li, 3.5	0.374	300	1400	2.0	15.1	15.86	10.66	5.82	4.27

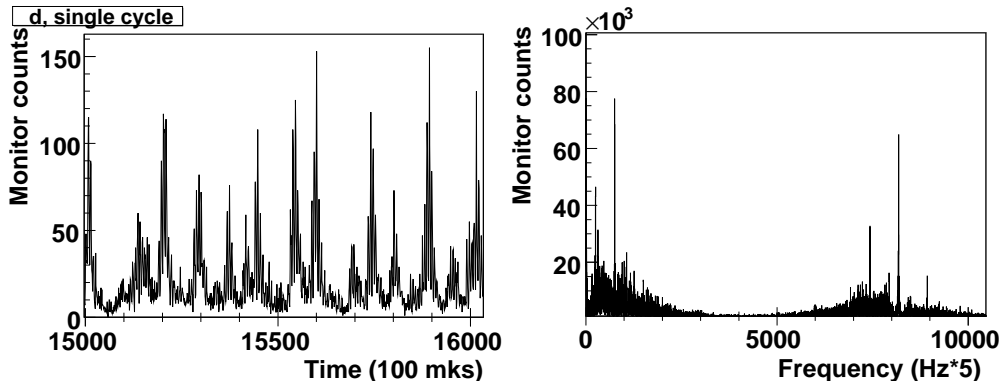


Figure 4: The monitor counts in the 0.1 s window (left) and Fourier transform of the full burst (right) during the single cycle from the slowly extracted deuteron beam of $T_{\text{kin}} = 3.5$ A·GeV in F6 focus. See text for description.

Table 3: Nuclotron internal beam–target interaction characteristics. The time limits for the K_{dc} (see equation (1)) calculations are: $t_1 = 1000$ ms, $t_2 = 3500$ ms. The frequency ranges for the mechanical vibrations of the internal target (Δf_{ITS}) are 12..14 Hz for C and 13..15 Hz for CH₂.

Beam, T_{kin} (A·GeV)	Target	K_{dc}	$\frac{\Delta N(\Delta f)}{0.5 N_{\text{tot}}}$ (%) for Δf as $f_1..f_2$ (Hz)				
			0..1	Δf_{ITS}	49..51	99..101	149..151
d, 0.25	CH ₂	0.56	13.0	3.2	7.9	4.4	1.5
d, 0.25	C	0.82	19.5	1.1	1.0	0.26	0.08
d, 3.5	CH ₂	0.926	32.0	5.4	5.4	0.6	0.35
d, 3.5	C	0.918	30.1	0.9	5.9	1.1	0.53

per mean are calculated and printed to standard error output. The *b2h(1) listen(2)s* on port 12342 for the client registration. For each registered client the *b2h(1)* sends all histograms by *TMessages* once per cycle. Also all configured histograms are written optionally to ROOT *TFile* periodically or at *b2h(1)* termination as well as at *SIGHUP* signal obtaining. The *SIGINT* signal resets all histograms, *SIGUSR1* and *SIGUSR2* switches to read-and-discard mode and vice versa. For user termination in accuracy manner the *SIGTERM* signal should be used.

The ROOT script *client5.C* connects to *b2h(1)* server, obtains TH1F histograms encoded into *TMessages*, and draws each of them in separate *TCanvases*. To allow the full user interaction with these histograms the script should be terminated (i.e., by twice *<Ctrl><C>* pressing), because the proper coexistence of two endless loops (for *TSocket* reading and X11 [24] events handling) could be managed only in the executable like *histGUI(1)* [20].

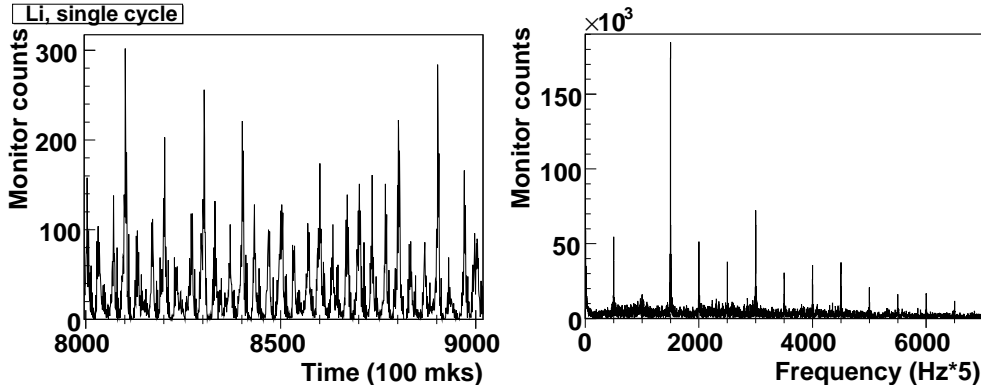


Figure 5: The monitor counts in the 0.1 s window (left) and Fourier transform of the full burst (right) during the single cycle from the slowly extracted ${}^7\text{Li}$ beam of $T_{\text{kin}} = 3.5 \text{ A}\cdot\text{GeV}$ in F4 focus. See text for description.

2 Nuclotron extracted beam results

The first setup version was implemented in 2009 and successfully used during 7 Nuclotron runs in 2011–2015 to measure the extracted deuteron, carbon, and ${}^7\text{Li}$ beams time structure. The scintillation counter ($100 \times 40 \times 4 \text{ mm}^3$) with XP2020Q PMT movable by motor was situated in the beam halo near the F4 focus of the VP1 transport beamline. The PMT pulses shaped by 4F-115 discriminator were used as the input monitor counts for the setup.

The measurements were performed during the data taking on the measurements of the soft photons yield [13]. The typical averaged number of the counts in the $100 \mu\text{s}$ time slice was 28, 24 and 7 per beam spill for the ${}^7\text{Li}$, deuteron and carbon beam, respectively. In Figs. 4–6 the typical monitor counts proportional to the beam-target interaction rate during a single cycle are shown for the beam of deuterons, ${}^7\text{Li}$, and carbon with 3.5 A·GeV kinetic energy. The abscissa is a time bin number, the ordinate is the number of counts in the corresponding bin. The bin width is equal to the time slice, $100 \mu\text{s}$. The typical 0.1 s time windows are shown on the right panels instead of the full burst timescale. The K_{dc} value (see equation (1)) could be obtained easily from these data in online or offline. For the single cycles depicted in Figs. 4–6 the K_{dc} during the full burst time ($t_2 - t_1$) are represented in Table 2. We are not show the whole run (per-bin cumulative sum) histograms because the single cycle statistics is large enough. The Fourier transforms of the corresponding full burst statistics are shown in Figs. 4–6 on the left panels. As one can see, some frequencies (50 Hz and harmonics) are emphasized. Their origin is a time structure of the slowly extracted beam. The ratio $\frac{\Delta N(\Delta f)}{0.5N_{\text{tot}}}$ values for some set of frequency ranges $\Delta f = f_2 - f_1$ (in Hz) are represented in Table 2. The K_{dc} coefficient is smaller than 0.5. This reflects the large width of the frequency spectrum (see right panels in Figs. 4–6). On the other hand, the contribution of the harmonics proportional to 50 Hz is lower than 7 % in the worst case of ${}^7\text{Li}$. One can conclude, that significant improvement of the extracted beam time structure is required for the high intensity experiments, for instance, by the feedback from the monitor counter to the accelerator.

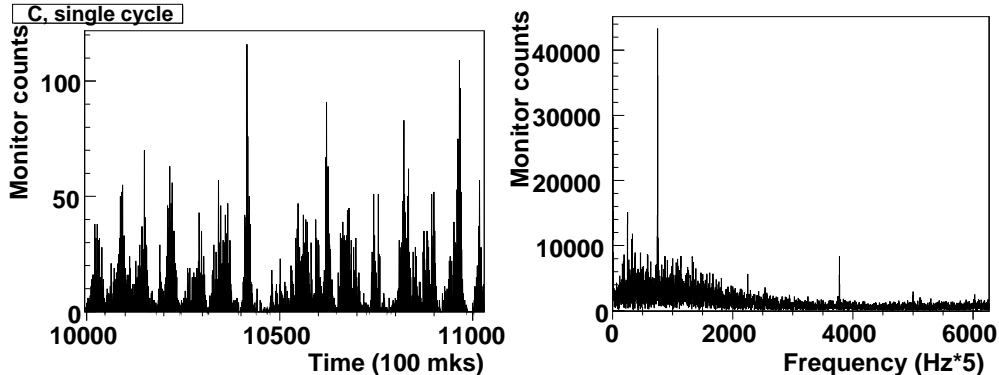


Figure 6: The monitor counts in the 0.1 s window (left) and Fourier transform of the full burst (right) during the single cycle from the slowly extracted ^{12}C beam of $T_{\text{kin}} = 3.5$ A·GeV in F6 focus. See text for description.

3 Nuclotron internal beam results

The second setup version for the Nuclotron internal beam was implemented in 2014 and successfully used during 2 Nuclotron runs (June'2014 and March'2015) to measure the time scans of the beam-target interactions in the accelerator ring. The scintillation counter ($100 \times 100 \times 4$ mm³) with FEU-30 PMT observes the beam-target interaction point of the Nuclotron internal target station (ITS) [12] from 1 m distance under 60° angle in horizontal plane to produce the input monitor counts for both ITS and current setup DAQ systems. The analog signal from PMT with the rising time of ~ 5 ns and total duration of ~ 15 ns is shaped by the 4F-115 discriminator with ~ 40 mV threshold. The duration of the output pulse is ~ 100 ns. In the second setup version the counting is started by hardware at the same time offset for each cycle (with ≈ 50 ns uncertainty) after the BoB event occurrence. This allows us to work with the whole run histograms because the subtle counting start variation in time can not “smudge” the time structure on such additive picture.

The quality of the electronic chain has been checked using ^{106}Ru radioactive (RA) source. The Fourier transform of the monitor counts from the ^{106}Ru RA source is shown on the left panel in Fig. 7 for the whole run. These data were obtained while the 150 A·MeV deuteron beam was accelerated and circulated in the Nuclotron ring, however the internal target was not run. The averaged number of counts in the $100 \mu\text{s}$ time slice is ~ 15 . The data demonstrate white noise picture that proofs the quality of the used electronic chain. The right panel in Fig. 7 shows the Fourier transform of the monitor counts from both the deuterons of the same energy on CH_2 target and the ^{106}Ru RA source simultaneously. The frequencies corresponding to target mechanical vibrations and to the $n \cdot 50$ Hz harmonics are clearly seen.

The data on the deuteron beam time structure were obtained simultaneously with the data taking for the DSS experiment [3] with $10 \mu\text{m}$ CH_2 foil and $8 \mu\text{m}$ carbon multiwire targets with the typical intensity of $5 \div 8 \cdot 10^8$ deuterons per spill. The typical averaged number of the counts in the $100 \mu\text{s}$ time slice was ~ 15 and ~ 180 per spill at the beam

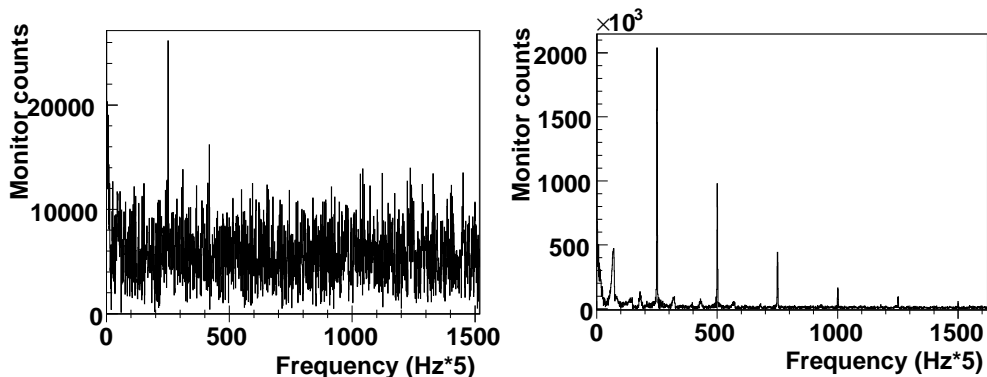


Figure 7: The Fourier transform of the monitor counts from the ^{106}Ru radioactive source without (left) and with (right) Nuclotron internal deuteron beam of $T_{\text{kin}} = 150 \text{ A}\cdot\text{MeV}$ on the CH_2 target for the whole run. See text for description.

energy of 250 A·MeV and 3.5 A·GeV, respectively.

In Figs. 8 and 9 we can see the full burst timescale (left panels) of the monitor counts during the whole run (per-bin cumulative sum) from the beam of deuterons with 250 A·MeV kinetic energy interacting with the CH_2 and C targets, respectively. The Fourier transforms of the corresponding full burst statistics for the CH_2 and C target are shown in Figs. 8 and 9 on right panels. The same for the 3.5 A·GeV deuteron beam is shown in Figs. 10 and 11. One can see some frequencies (50 Hz and harmonics) other than originated from the mechanical target vibrations are enhanced, however their relative intensity is decreased with the frequency increasing. Their origin can be a space-time structure of the Nuclotron internal beam. The ratio $\frac{\Delta N(\Delta f)}{0.5N_{\text{tot}}}$ values for some set of enhanced frequencies f in narrow ranges $\Delta f = f \pm 1 \text{ Hz}$ are represented in Table 3. The “ Δf_{ITS} ” column contains this ratio for mechanical vibrations frequency of the internal target ($\approx 13 \text{ Hz}$ for C and $\approx 14 \text{ Hz}$ for CH_2 in the represented data). The results confirm the earlier observation [12] that the mechanical vibrations are larger for CH_2 target. The K_{dc} coefficient is ~ 0.9 at 3.5 A·GeV for both targets. The contribution of the $n \cdot 50 \text{ Hz}$ harmonics is only about $8 \div 10 \%$. However we observe the significant difference in K_{dc} coefficient and contribution of the $n \cdot 50 \text{ Hz}$ harmonics for CH_2 and C targets at low energies. For carbon target the $K_{\text{dc}} \sim 0.8$ and the $n \cdot 50 \text{ Hz}$ harmonics contribution is only 1.5 %. Therefore, one can conclude that the time structure of the internal beam interaction with carbon target allows one to perform experiments at ITS. For CH_2 target the K_{dc} is only 0.56 and the $n \cdot 50 \text{ Hz}$ harmonics contribution is $\sim 15 \%$. The reason of this difference is the subject of further studies.

Conclusions

The results of the present work can be summarized as follows:

- Two similar setups for precise measurements of the Nuclotron beam time structure are designed using standard CAMAC modules produced at LHEP and DLNP. They are commissioned for the experiments at internal target and at the slowly extracted beam.

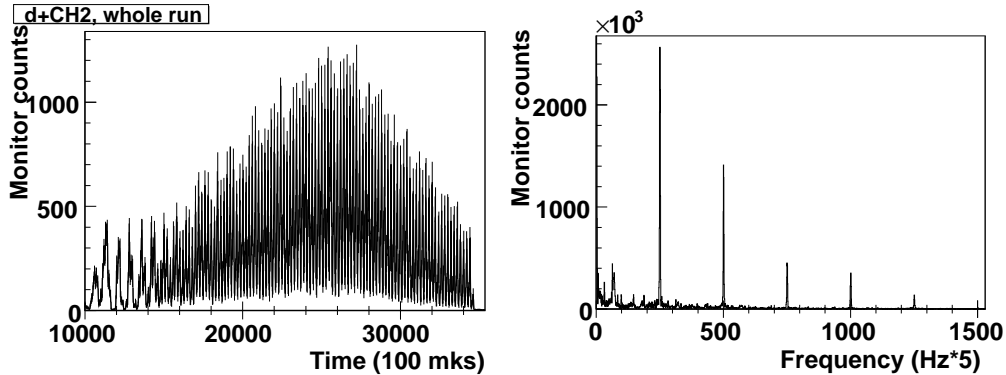


Figure 8: The monitor counts during the whole run (left) and their Fourier transform (right) for Nuclotron internal deuteron beam of $T_{kin} = 250$ A·MeV on the CH₂ target. See text for description.

Both setups are working with the 100 μ s time slices, so they are able to investigate the frequency domain up to ≈ 4.5 kHz.

- The data on the beam time structure could be easily distributed online through network on the cycle-by-cycle basis due to Spill DAQ design on base of the *ngdp* framework [19, 20]. Therefore, these setups are suitable to work continuously during the whole Nuclotron run and provide data for the beam quality estimations.
- The first setup version was successfully used to measure the time structure of the slowly extracted beam of deuterons, ⁷Li, and carbon at 3.5 A·GeV.
- The second setup version was used to measure the time structure of the beam-target interaction inside the Nuclotron ring at ITS [11, 12]. It has been found the influence of the mechanical vibrations of the internal target on the data taking.
- The developed setups can be efficiently used as a tool for the permanent monitoring of the Nuclotron beam quality during the experiments performed at Nuclotron.

Acknowledgments

The authors have the pleasure to thank Prof. L.S.Zolin for initiation of this work, cooperation during measurements, and permanent interest to results, the Nuclotron team and in particular Dr. A.V.Butenko — for fruitful cooperation. The authors are grateful to A.N. Livanov, S.M. Piyadin, and A.N. Khrenov for the technical support during the measurements at internal target. The present work was supported in part by the RFBR Grant no.13-02-00101a.

References

- [1] *Ablyazimov T.O. et al.* (BM@N Collaboration). Conceptual Design Report of BM@N. Dubna: JINR, 2012.

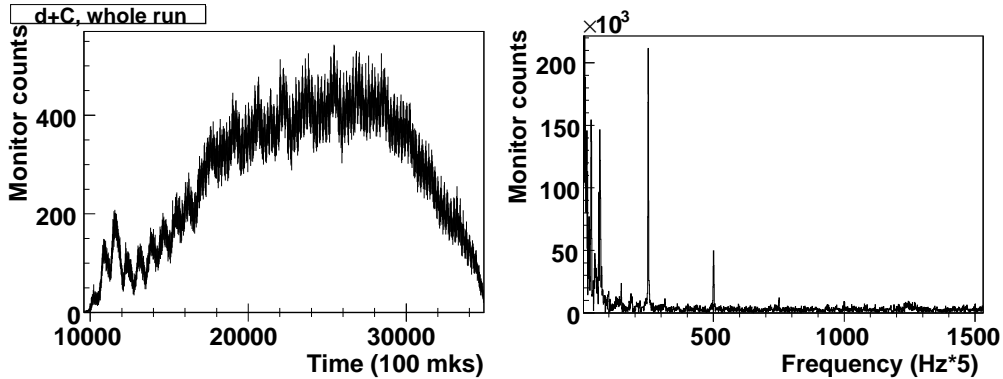


Figure 9: The monitor counts during the whole run (left) and their Fourier transform (right) for Nuclotron internal deuteron beam of $T_{\text{kin}} = 250$ A·MeV on the C target. See text for description.

- [2] *Ladygin V. P. , Ablyazimov T. O., Aichelin J., et al.* Study of strange matter production in the heavy ion collisions at Nuclotron. // Proceedings of XXI Intern. Seminar on High Energy Physics Problems (ISHEPP'2012), Dubna, Russia, 2012. PoS 038, 2012. P. 1–8.
- [3] *Ladygin V.P., Gurchin Yu.V., Piyadin S.M., Terekhin A.A., Isupov A. Yu., et al.* Few-body Studies at Nuclotron-JINR. // Few Body Systems. 2014. V. 55. P. 709–712.
- [4] *Ladygin V.P. et al.* Spin physics in few body systems at Nuclotron. // Particles and Nuclei. 2014. V. 45. P. 327.
- [5] *Ladygin V.P.* Polarization effects in hadronic reactions in a GeV region. // Proceedings of XXII Intern. Seminar on High Energy Physics Problems (ISHEPP'2014), Dubna, Russia, 2014. PoS 098, 2012. P. 1.
- [6] *Ladygin V.P.* Dead-time distortion in polarization measurements. // Nucl.Instr.and Meth.in Phys.Res.A. 1999. V. 437. P. 98.
- [7] *Kurilkin P.K. et al.* Measurement of the vector and tensor analyzing powers for dp -elastic scattering at 880 MeV. // Phys.Lett.B. 2012. V. 715. P. 61.
- [8] *Kurilkin P.K. et al.* Investigation of the angular dependence of the analyzing powers in the deuteron-proton elastic scattering at the nuclotron. // Particles and Nuclei, Letters. 2011. V. 8. P. 1081.
- [9] *Azhgirey L.S. et al.* Observation of tensor polarization of deuteron beam traveling through matter. // Particles and Nuclei, Letters. 2008. V. 5. P. 728–735.
- [10] *Azhgirey L.S. et al.* Measurement of tensor polarization of a deuteron beam passing through matter. // Particles and Nuclei, Letters. 2010. V. 7. P. 27.

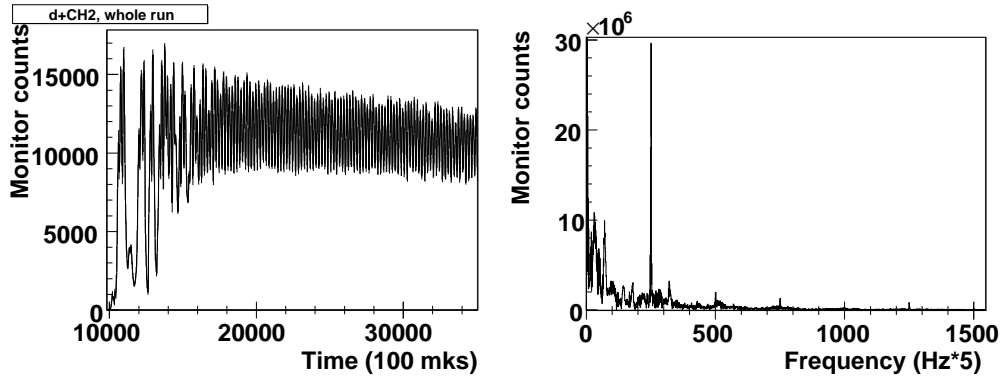


Figure 10: The monitor counts during the whole run (left) and their Fourier transform (right) for Nuclotron internal deuteron beam of $T_{\text{kin}} = 3.5$ A·GeV on the CH₂ target. See text for description.

- [11] *Malakhov A.I. et al.* Potentialities of the internal target station at the Nuclotron. // Nucl.Instr.and Meth.in Phys.Res.A. 2000. V. 440. P. 320–329.
- [12] *Isupov A. Yu., Krasnov V. A., Ladygin V. P., Piyadin S. M., and Reznikov S. G.* The Nuclotron Internal Target Control and Data Acquisition System. // Nucl. Instr. and Meth. in Phys. Res. A. 2013. V. 698. P. 127–134.
- [13] *Aleev A. et al. (SVD Collaboration).* Study of pp Interactions at U-70. // Nonlin. Phenom. Complex Syst. 2014. V. 17. P. 448–450.
- [14] <http://afi.jinr.ru/VMEDAQ> , 2012.
- [15] *Churin I. and Georgiev A.* // Microprocessing and Microprogramming. 1988. V. 23. P. 153.
- [16] *Antyukhov V.A. et al.* The digital CAMAC modules. Issue V (in Russian). JINR Commun. 10–10576. Dubna, 1977. P. 14.
- [17] *Gritsaj K. I. and Olshevsky V. G.* Software package for work with CAMAC in Operating system FreeBSD (in Russian). // JINR Commun. P10–98–163. Dubna, 1998. 16 p.
- [18] <http://www.freebsd.org/cgi/man.cgi?query=netgraph&sektion=4> , 2008.
- [19] *Isupov A. Yu.* The *ngdp* framework for data acquisition systems. arXiv:1004.4474 [physics.ins-det], 2010. 20 p.
- [20] *Isupov A. Yu.* CAMAC subsystem and user context utilities in *ngdp* framework. arXiv:1004.4482 [physics.ins-det], 2010. 20 p.
- [21] *Gritsaj K. I. and Isupov A. Yu.* A Trial of Distributed Portable Data Acquisition and Processing System Implementation: the *qdpb* – Data Processing with Branchpoints. // JINR Commun. E10–2001–116. Dubna, 2001. 19 p.

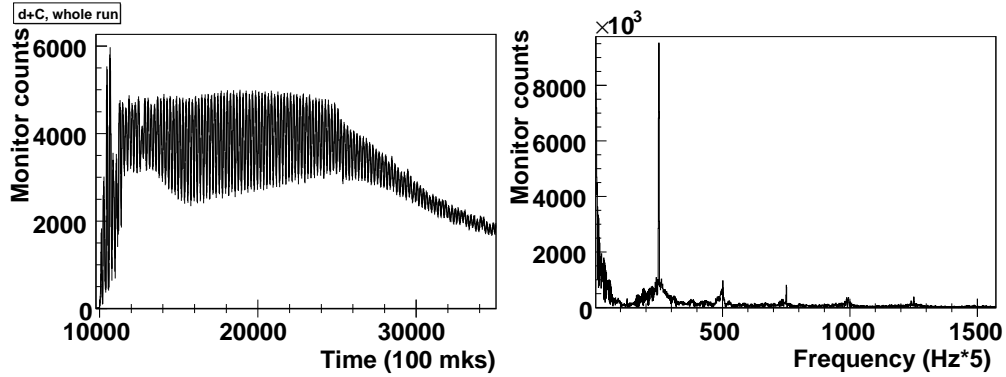


Figure 11: The monitor counts during the whole run (left) and their Fourier transform (right) for Nuclotron internal deuteron beam of $T_{\text{kin}} = 3.5 \text{ A}\cdot\text{GeV}$ on the C target. See text for description.

- [22] *Brun R. and Rademakers F.* ROOT – An Object Oriented Data Analysis Framework. // Proc. of the AIHENP'96 Workshop, Lausanne, Switzerland, 1996. Nucl.Instr.and Meth.in Phys.Res.A. 1997. V. 389. P. 81–86.
- [23] *Isupov A. Yu.* SPHERE DAQ and off-line systems: implementation based on the *qdpb* system. // JINR Commun. E10–2003–187. Dubna, 2003. 17 p.
- [24] Volume 0: X Protocol Reference Manual. / Ed.: Adrian Nye. 3rd ed. N.-Y.: O'Reilly & Associates, 1992.